See related commentary on pg 499

5′ *Trans*-Splicing Repair of the *PLEC1* Gene

Verena Wally[1], Alfred Klausegger[1], Ulrich Koller[1], Hanns Lochmüller[2], Sabine Krause[2], Gerhard Wiche[3], Lloyd G. Mitchell[4], Helmut Hintner[1] and Johann W. Bauer[1]

The efficient treatment of hereditary disorders, especially of those caused by dominant-negative mutations still remains an obstacle to be overcome. Allele specificity is a critical aspect that must be addressed by silencing therapies such as small interfering RNA, which has the potential risk of also reducing expression of the normal allele. To overcome this hurdle, we used spliceosome-mediated RNA *trans*-splicing (SMaRT) to replace mRNA exon segments in an *in vitro* disease model. In this model, a heterozygous insertion of a leucine codon into exon 9 of the plectin gene (*PLEC1*) leads to aggregation of plectin peptide chains and subsequent protein degradation recapitulating, together with a nonsense mutation on the other allele, the blistering skin disease epidermolysis bullosa simplex with muscular dystrophy (EBS-MD). Transient transfection of EBS-MD fibroblasts with a 5′ pre-*trans*-splicing molecule encoding wild-type exons 2–9 led to specific replacement of the mutated 5′ portion of the endogenous *PLEC1* transcript through *trans*-splicing. This treatment reduced the levels of mutant mRNA and restored a wild-type pattern of plectin expression as revealed by immunofluorescence microscopy. When EBS-MD fibroblasts were transfected with retroviral constructs, the level of full-length plectin protein in the corrected fibroblasts increased by 58.7%. Thus, SMaRT may be a promising new tool for treatment of autosomal-dominant genetic diseases.

Journal of Investigative Dermatology (2008) **128,** 568–574; doi:10.1038/sj.jid.5701152; published online 8 November 2007

INTRODUCTION

Reprogramming of pre-mRNAs by means of spliceosome-mediated RNA *trans*-splicing (SMaRT) is based on exploiting the naturally occurring splicing events required for pre-mRNA maturation (Puttaraju *et al.*, 1999). SMaRT utilizes the endogenous splicing machinery to recombine two independent RNA molecules by *trans*-splicing, replacing the disease-causing portion of a pre-mRNA with an engineered sequence in an exon-specific manner. These reactions are affected by engineered pre-*trans*-splicing molecules (PTMs) that contain a binding region to base pair specifically with the targeted intron of a pre-mRNA, thus facilitating *trans*-splicing between the PTM and the target pre-mRNA. In this case, the PTM brings in the wild-type coding region to be *trans*-spliced to the target using a functional 5′ splice site.

Trans-splicing can replace either the 3′, 5′, or internal exon(s) of the pre-mRNA target, referred to as 3′-, 5′-, or internal exon replacement. Of these methods, the 3′ *trans*-splicing strategy is the most commonly used. 5′ *trans*-splicing has been used in a double transfection experiment to reprogram mutations in plasmid-encoded cystic fibrosis transmembrane receptor (CFTR) and β-globin genes (Mansfield *et al.*, 2003; Kierlin-Duncan and Sullenger, 2007), but has not been reported for an endogenous gene target at this time. Successful and safe 3′ *trans*-splicing therapy has been demonstrated in animal models of autosomal-recessive genetic diseases such as cystic fibrosis, X-linked immunodeficiency, and hemophilia (Liu *et al.*, 2002; Chao *et al.*, 2003; Tahara *et al.*, 2004).

Several advantages of *trans*-splicing have been considered in the past. First, the natural expression pattern of the target gene is retained. Second, the segmental introduction of therapeutic molecules allows much smaller correcting molecules to be used (for a review see Chao and Walsh, 2006). Third, *trans*-splicing converts the mutant allele to wild type, thereby not only knocking down expression of a mutated allele, but also increasing the level of normal protein beyond that provided by simply ablating the mutant form. This makes it especially appealing for dominant-negative mutations. However, no experimental evidence has been shown yet for this third point.

After considering the disadvantages of specificity, efficiency, safety, and sequence limitations associated with other possible nucleotide therapeutic approaches (such as RNAi,

[1]*Division of Molecular Dermatology and eb house Austria, Department of Dermatology, Paracelsus Private Medical University, Salzburg, Austria;* [2]*Department of Neurology, Friedrich-Baur-Institute, Ludwig-Maximilians-University of Munich, Munich, Germany;* [3]*Max F. Perutz Laboratories, Vienna Biocenter, Institute of Biochemistry and Molecular Cell Biology, University of Vienna, Vienna, Austria and* [4]*Retrotherapy LLC, Bethesda, Maryland, USA*

Correspondence: Professor Johann W. Bauer, Division of Molecular Dermatology and eb house Austria, *Department of Dermatology, Paracelsus Private Medical University Salzburg, Muellner Hauptstrasse 48, 5020 Salzburg, Austria. E-mail: jo.bauer@salk.at*

*Abbreviations: BD, binding domain; cDNA, complementary DNA; CFTR, cystic fibrosis transmembrane receptor; CFU, colony forming units; EBS-MD, epidermolysis bullosa simplex with muscular dystrophy; PLEC1, plectin gene; PTM, pre-*trans*-splicing molecule; SMaRT, spliceosome-mediated RNA* trans*-splicing; SQRT-PCR, semiquantitative real-time PCR*

Received 14 February 2007; revised 6 September 2007; accepted 7 September 2007; published online 8 November 2007

ribozymes, and antisense), we chose to develop SMaRT as a potential treatment of mutation in large genes that act in a dominant-negative manner.

We used cells from patients suffering from epidermolysis bullosa as a model system to study the 5′ SMaRT approach. Mutations in the plectin gene (*PLEC1*) underlie epidermolysis bullosa simplex with late onset muscular dystrophy (EBS-MD). At 14.2 kb, *PLEC1* produces one of the largest known mRNAs and exceeds the packaging capacity of most viral vectors. *PLEC1* encodes a large cytolinker protein that anchors and connects the keratinocyte cytoskeleton to the hemidesmosomes. The skin and muscles of patients with EBS-MD are (severely) affected by the fragility of the mutated cellular anchoring structures, leading to the development of blisters and skin erosions. In this study, we used cells derived from a compound heterozygous patient with a 3 bp insertion in exon 9 (1287ins3) and a nonsense mutation in exon 31 (Q1518X) of the *PLEC1* gene. The insertion of a CTG in position 1287 leads to the incorporation of an additional leucine at position 429 on protein level, which increases the hydrophobicity in this region and may lead to changes in conformation. A previous study showed that this additional leucine residue promotes self-aggregation, resulting in the degradation of full-length plectin protein in the presence of unaltered PLEC1 mRNA levels. This molecular constellation (i.e., preserved mRNA expression levels, but a protein product produced by one allele affecting the overall function of the molecule) can also be seen in dominantly inherited forms of EB, EB simplex, and dystrophicans. This mechanism allows us to use these patient-derived cells as a model for a dominant-negative gene product (Bauer *et al.*, 2001). On the basis of these considerations, we transduced EBS-MD cells with a PTM designed to repair any mutation in the 5′ coding region of the *PLEC1* gene and demonstrated the applicability of *trans*-splicing for the treatment of hereditary diseases of the skin.

RESULTS

Endogenous *trans*-splicing in the PLEC1 gene

Primary fibroblasts derived from an EBS-MD patient heterozygous for the *PLEC1* mutations 1287ins3/Q1518X were immortalized to prevent senescence of the cells during the experimental procedures. The immortalized cells were morphologically indistinguishable from both normal fibroblasts and untreated cells from the patient. Furthermore, the presence of the insertion mutation in exon 9 of the immortalized cells was confirmed by sequencing (data not shown). A PTM-E50 was designed to contain features specific to 5′ *trans*-splicing (Figure 1; Mansfield *et al.*, 2003). These are as follows: (i) a 50-bp binding domain complementary to both the last 40 nucleotides of intron 9 of the targeted plectin pre-mRNA and the first 10 nucleotides of exon 10; (ii) a 183-bp spacer region; (iii) the wild-type plectin exons 2–9, which encompass 1026 nt (exon 1 is an alternative exon); (iv) the functional plectin intron-9 5′ splice site and an intronic splicing activator and repressor sequence; (v) a cytomegalovirus promoter and an SV40 polyadenylation signal. The plasmid expressing this PTM was transiently transfected into immortalized patient fibroblasts to test for *trans*-splicing repair of endogenous plectin mRNA. Levels of normal and mutant plectin mRNA were measured by semiquantitative real-time PCR (SQRT-PCR), amplifying complementary DNA (cDNA) from wild-type fibroblasts, transfected and non-transfected EBS-MD fibroblasts. A wild-type specific forward PCR primer was designed to discriminate between wild-type and mutated mRNA molecules by inclusion of the four wild-type gct repeats in exon 9. The reverse primer was complementary to *PLEC1* exon 10 (Figure 2a). Analysis of the PCR products from wild-type fibroblasts showed the expected 189-bp band, representing the wild-type allele. After transient transfection with PTM-E50, wild-type plectin cDNA levels were increased by an average of 83.42% as

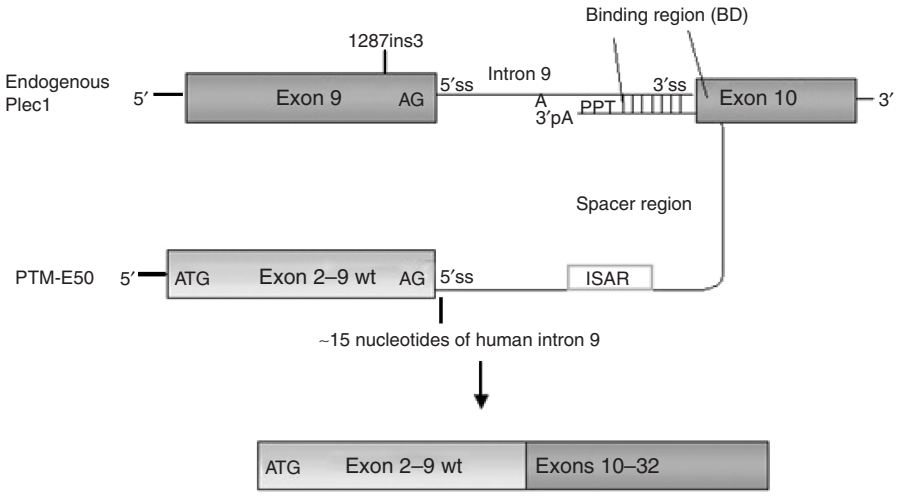

Figure 1. Schematic depiction of the endogenous target in EBS-MD cells and the PTM-E50. The binding region (BD) is complementary to the last 40 bases of intron 9 and the first 10 bases of exon 10 of the endogenous target plectin pre-mRNA. *Trans*-splicing results in a mature corrected mRNA combining wild-type exons 2–9 brought in by the PTM, and exons 10–32 of the endogenous *PLEC1* target pre-mRNA. ISAR, intronic splicing activator and repressor; PPT, polypyrimidine tract; 5′ and 3′ ss, splice sites.

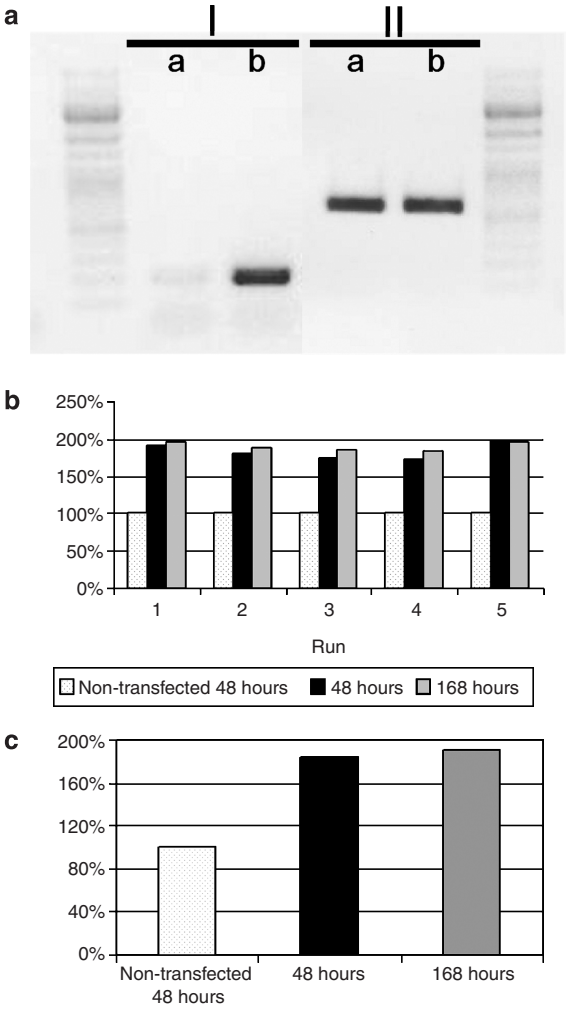

Figure 2. Real-time PCR of transfected patient cells. (**a**) A specific primer amplifies the wild-type strand only. I: PCR using the wild-type-specific forward primer (see Materials and Methods) in combination with a reverse primer specific to exon 10. Lane a: PCR of patient cDNA encompassing position 1026. Lane b: cDNA from an unaffected person. II: As a reference, the same amount of cDNA was used for PCR with primers specific to the housekeeping gene *GAPDH*. (**b**) SQRT-PCR showing an increase of the wild-type mRNA in PTM-transfected versus -non-transfected EBS-MD fibroblasts. Five SQRT-PCR runs of three independent transfection experiments are shown. (**c**) A mean increase of the wild-type allele of 83.42% after 48 hours was detected.

measured by SQRT-PCR in four independent experiments (Figure 2b and c).

Specificity of *trans*-splicing determined by cross-gene PCR

Members of the plakin gene family, including plectin, show high sequence homology, thus constituting a model group of genes to evaluate illegitimate, nonspecific PTM *trans*-splicing. PCR primers were designed to amplify exons flanking sequences with the highest homology to the PTM-binding domain for six plakin family genes desmoplakin, envoplakin, epiplakin, dystonin, periplakin, and microtubule-actin crosslinking factor 1. Cross-gene PCR between these plakin family genes and exon 9 of *PLEC1* was performed.

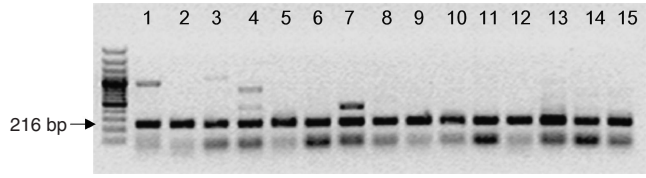

Figure 3. Cross-gene PCR analysis for plectin and related plakin genes showed specificity of the 5′ trans-splicing process. We detected no specific bands except for the plectin control (216 bp) in PTM-R50-infected patient cells. Some nonspecific bands (lanes 1, 3, 4, and 7) also occurred in the non-transfected EBS-MD fibroblasts (data not shown). Thus they can be regarded as nonspecific PCR products. Lane 1: reverse primer for desmoplakin; lanes 2–8, microtubule-actin crosslinking factor 1; lanes 9–11, dystonin; lane 12, epiplakin; lane 13, envoplakin; lanes 14 and 15, periplakin.

These PCRs revealed only the expected plectin-specific control band at 216 bp (Figure 3). Some nonspecific PCR bands were produced, which were also detected in the cross-gene PCR analysis of non-transfected patient fibroblasts, using the same primers. Nonspecific bands were cloned into TOPO-TA and sequenced, confirming them not to be nonspecific *trans*-splicing products but nonspecific PCR products. These results demonstrate a high level of 5′ *trans*-splicing specificity in the plakin gene family.

Plectin repair restores the expression of plectin-containing structures

Wild-type fibroblasts display intense plectin staining throughout the cytoplasm (Figure 4a). Previous studies of EBS-MD cells from a distinct family showed increased self-aggregation of mutant plectin polypeptides by an *in vitro* overlay assay (Bauer *et al.*, 2001). These aggregates were also visualized in the cytoplasm of untreated patient fibroblasts (Figure 4c) by immunofluorescence-optical analysis using the plectin-specific mAb 5B3 (Foisner *et al.*, 1994). In cells transiently transfected with PTM-E50, we observed the generation of the characteristic plectin-containing structures as well as a reduction of aggregates in about 30% of the cells (Figure 4b).

PTM-R50 delivered by a retroviral vector generates expression of full-length plectin protein

To test the feasibility of retroviral delivery, we cloned the PTM into the retroviral vector pLXSN (PTM-R50). PTM-R50 was transfected into the host cell line PT67 and virus was produced following the manufacturer's protocol. Positive supernatants were used for viral titer determination (Figure 5). Five-hundred microliters of PTM-R50-positive viral supernatant (VS1) with a titer of 2×10^6 colony forming units (CFU) per ml were used for the infection of 2×10^6 primary EBS-MD fibroblasts. The expression of full-length plectin protein was evaluated by western blot analysis. Total protein was extracted from VS1-infected EBS-MD fibroblasts after 3 days of culture without G418 selection to avoid geneticin-associated readthrough of the stop codon Q1518X on the second allele. A ~500 kDa band was detected in samples from infected cells and comigrated with the plectin protein band of wild-type fibroblasts. This band was only 18.22% in

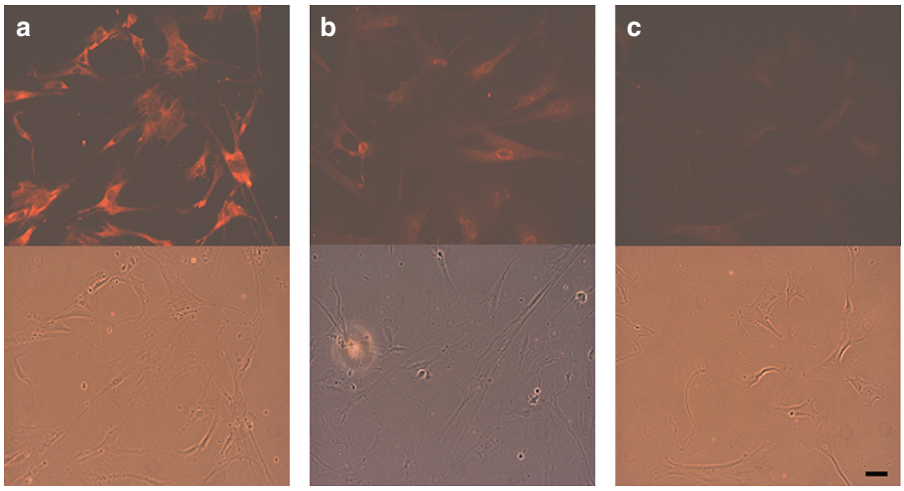

Figure 4. Restoration of plectin protein expression in PTM-E50-transfected EBS-MD fibroblasts detected by immunofluorescence. Immunofluorescence pictures and corresponding light microscopy pictures are shown. (**a**) Wild-type fibroblasts. (**b**) Representative EBS-MD fibroblasts transiently transfected with PTM-E50. (**c**) Non-transfected (mutant) EBS-MD fibroblasts. Bar = 10 μm.

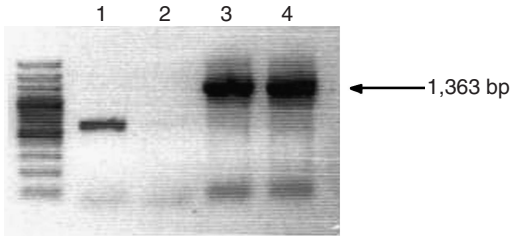

Figure 5. RT-PCR products of viral supernatant (VS1) of RetroPack PT67 cells transfected with PTM-R50. A PCR product of 1363 bp represents the correct insert length (lane 4). Lanes 1 and 3 are positive controls for *GAPDH* and PTM-R50, respectively. Lane 2 shows the results of a PCR designed to amplify *GAPDH* from genomic DNA as a test for genomic DNA contamination of the viral supernatant.

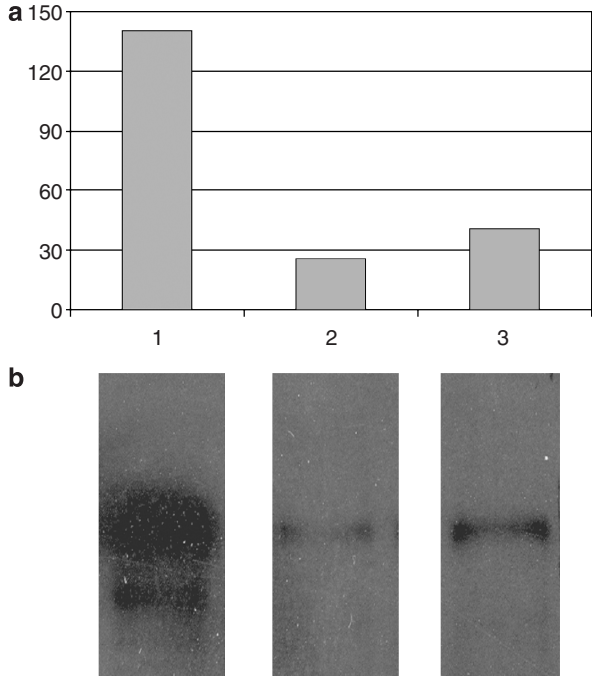

Figure 6. Restoration of full-length plectin protein in western blotting. (**a**) Bars show relative amounts of plectin analyzed by densitometric scanning. (**b**) Lane 1: protein from wild-type human fibroblasts showing the expression of full-length plectin protein. Non-infected EBS-MD fibroblasts (lane 2). Production of full-length plectin protein (lane 3) in EBS-MD fibroblasts infected with viral supernatant containing PTM-R50 for 2 days without selection. One representative blot of three experiments is shown.

non-transfected EBS-MD cells compared to wild-type fibroblasts and increased to 28.93% in infected cells, as detected by densitometric measurements. This means an increase of 58.78% of full-length plectin protein in total protein extracts of infected fibroblasts compared to non-infected fibroblasts (Figure 6a and b). This increase roughly correlates also with the results of the SQRT-PCR.

DISCUSSION

In this study, we demonstrate 5′ SMaRT to be a functional tool for the correction of any mutation in an upstream part of an affected gene/allele.

Using SMaRT *trans*-splicing-based RNA therapy, a defined endogenously expressed target pre-mRNA is cleaved and a new sequence from a *trans*-splicing molecule is inserted either upstream, downstream, or within the selected target to generate a new gene product. Expression of the *trans*-spliced gene is regulated by the cellular control elements and the presence of the target gene. *Trans*-splicing efficiencies as high as 50% have been achieved in studies targeting endogenous human papilloma virus pre-mRNAs in cultured cells from cervical cancers (unpublished data). Functional restoration of up to 22% of normal chloride channel activity has been achieved in a cystic fibrosis xenograft model. This is a level that could provide therapeutic benefit in the treatment of a significant number of diseases (Liu *et al.*, 2002). In human

skin cells, we have been able to detect up to 24% *trans*-splicing efficiency in a 3′ SMaRT approach (Dallinger *et al.*, 2003).

In the transient transfection assays reported here, 30% of the EBS-MD cells were plectin-positive by immunofluorescence microscopy 7 days after the transfection. Cells that were positive showed plectin-specific cytoskeletal staining features (Figure 4). Differences in the staining pattern compared with wild-type fibroblasts are due to a reduced amount of plectin protein expressed and a different cellular distribution due to isoform variations. We used plectin exons 2–9, skipping the alternative exon 1, which is cell type-specific. Inclusion of exon 1 leads to the expression of an additional actin and ITGB4-binding site, explaining variations in the staining pattern (Rezniczek *et al.*, 2003).

These data were corroborated by the western blot analysis of treated patient fibroblasts. Taking into account a correction of 10% of unselected retroviral-PTM-infected cells, the 58.78% increase in plectin expression detected in the PTM-treated cells as suggested by densitometric measurements implies that plectin levels should increase by more than 500% in retroviral-PTM-transduced cells after selection. However, G418 selection causes geneticin-associated stop codon readthrough (Lai *et al.*, 2004), rendering the contribution of *trans*-splicing to the overall corrective effect unclear if selection is employed.

Regardless of these technical considerations, for this technology to be useful in clinical applications, more efficient *trans*-splicing is needed. Although no nonspecific *trans*-splicing products were detected in our cross-gene evaluation of the plakin family of genes, optimization of PTM specificity might be necessary to achieve higher specific *trans*-splicing rates. This can be achieved by the use of high-capacity screening to identify the optimal binding sequence for the plectin gene followed by rational design, use of a tissue-specific promoter, and improvement in transgene delivery (Puttaraju *et al.*, 2004).

To date, most studies using SMaRT as a therapeutic approach to treat genetic diseases have focused on 3′ exon replacement. Recently, it was demonstrated that PTMs can also *trans*-splice the 5′ region of a transcript, replacing the 1.9-kb sequence coding for exons 1–10 of the *CFTR* gene or exon 1 of the β-globin gene (Mansfield *et al.*, 2003; Kierlin-Duncan and Sullenger, 2007). In the first study, a PTM plasmid was constructed to express a binding domain complementary to *CFTR* intron 10 along with a 5′ splice site and the coding sequences of *CFTR* exons 1–10. This was co-transfected in cultured human cells together with a target plasmid that expressed *CFTR* ΔF508 exon 10, a mini-intron 10 and exons 11–24. Full-length *trans*-spliced *CFTR* mRNAs (~6% of the *cis*-spliced target) and functional chloride ion channels were generated. Our results extend these studies by demonstrating 5′ exon replacement of an endogenous gene.

In summary, we have initiated the first gene therapeutic approach for plectin, one of the largest human genes with a 14.2 kb mRNA that far exceeds the capacity of current clinically approved viral vectors. With a single RNA *trans*-splicing construct, we demonstrated the capability to correct all possible mutations over a 1026-nt coding region of the *PLEC1* gene. Our results lead us to conclude that SMaRT may be a more cost-effective alternative for allele-specific treatment of genetic diseases, requiring the development, testing, and approval of far fewer products to treat a large number of different mutations. Furthermore, as *trans*-splicing does not involve the endogenous gene suppression pathways, it should have a different safety profile than the currently favored allele-specific gene therapy technology RNA interference, and hopefully fewer off-target effects.

MATERIALS AND METHODS

Immortalization of plectin-deficient (1287ins3/Q1518X) fibroblasts

Cells were infected with a retroviral vector carrying the E6 and E7 oncogenes (responsible for the promotion of cell proliferation and immortalization). Transformed cells were then selected for G418 resistance, pooled and maintained in G418-containing medium (Miller and Rosman, 1989).

Construction of PTMs

The mutation of interest is located in exon 9 at position 1287 (1287ins3) of the plectin gene (*PLEC1*). Therefore, the 5′ region of *PLEC1*, consisting of exons 2 (containing the initiation codon) to 9 of an unaffected person, was amplified by a one-step reverse transcriptase PCR (SuperScript One-Step RT-PCR with Platinum Taq; Invitrogen, Lofer, Austria). Exon 1 is a non-coding exon. A forward primer binding at the 5′ end of exon 2, which introduces a restriction site for cloning (gat**aagctt**gaggccatgtcggg) was used. To evaluate the functionality of the 3′ splice site of exon 9, a reverse primer with a 15-bp overhang was designed to introduce the first bases of intron 9 of *PLEC1* (shown in italicized letters) and a *Xho*I restriction site into the construct (gat**ctcgag***ccacggcaggcccac*tcaatctcctcgaagct).

Adjacent to the coding region of *PLEC1*, an intron was engineered comprising a binding domain (BD) complementary to intron 9 and the first 10 bases of exon 10 of *PLEC1*, thus bringing donor and acceptor splice sites into proximity, which may enhance *trans*-splicing. The first 10 bases of exon 10 were included into the PTM to theoretically block *cis*-splicing. In addition, an intronic splicing activator and repressor was introduced downstream of the PTM donor site, as it may enhance *trans*-splicing activity. PTM-E50 was cloned into pcDNA3.1D/V5-His-TOPO (Invitrogen). For stable transduction, PTM-R50 was subcloned into the retroviral vector pLXSN (PTM-R50) after introducing *Eco*RI and *Bam*HI restriction sites by PCR amplification (forward: GATGAATTCGA GGCCATGTCGGG, reverse: GATGGATCCCAACCACGCCGGGCTCT). Retroviral constructs were generated by digesting vector and insert with the appropriate restriction enzymes, gel purification, and ligation with T4 DNA ligase (New England Biolabs, Beverly, MA) overnight at 16°C, followed by transformation into the chemically competent *Escherichia coli* strain DH5α™-T1 (Invitrogen, Karlsruhe, Germany) and grown on lactose broth-ampicillin plates for selection. Cloning into the expression vectors was performed as suggested by the manufacturer's protocol (Invitrogen). Positive clones were identified by colony-PCR. The correct insert was confirmed by restriction digests and verified by DNA sequencing analysis.

Transient transfections

Human fibroblasts were grown in fibroblast basal medium (PromoCell, Heidelberg, Germany)/10% newborn calf serum (NCS) to ~80–90% confluency. The media was changed using antibiotic- and serum-free media; then the cells were transfected with 2–4 μg of plasmid (PTM-E50, pmaxGFP) using AMAXA Human Dermal Fibroblast Nucleofector kit (AMAXA GmbH, Germany). After incubation at 37°C for 48 hours and 7 days, respectively, cells were harvested for RNA and protein analysis.

Production of PT67 retroviral producer line using RetroX System (Clontech, Palo Alto, CA)

RetroPack PT67 cells were used for virus production. PTM-R50 or pLXSN (vector control) were separately transfected into the mouse NIH-3T3 fibroblast-derived cell line PT67 as described above. Virus production was performed according to the manufacturer's protocol. Several dilutions were plated to facilitate isolation of single colonies. After 3 days of growth, G418-containing medium was added to select for transfected cells. At the stage of 20–50 cells per colony, single colonies were picked and grown separately. After 14 days, cells were frozen and supernatants were analyzed by PCR (using vector-specific primers pLXSNfw and pLXSNrv; Clontech) and by sequence analysis for the presence of virus particles containing either the entire PTM-R50 or the empty vector.

Determination of viral titers

The infective potential of positive viral supernatants was tested by infecting NIH-3T3 mouse fibroblasts with six serial dilutions of the supernatants VS1, VS6, and VS24. After 3 days of growth, G418 was added to the medium to select for infected cells. An uninfected control plate was grown in parallel as a control. Cells were grown for another 14 days with a change of medium every other day. Viral titers were determined by counting the remaining colonies in the well with the highest dilution and multiplying by the dilution factor.

Infection of patient cells

Primary fibroblasts from an EBS-MD patient were grown to a confluency of 70%. Infection was performed as described by the manufacturer's protocol using the supernatant with the highest viral titer (VS1). After 48 hours, RNA and protein were isolated for analysis by real-time PCR and immunoblotting.

RNA preparation and RT-PCR

Total RNA was isolated using Epicenter MasterPure™ RNA Purification Kit (Epicenter Biotechnologies, Madison, WI). Contaminated plasmid and genomic DNA were eliminated by treating with DNase I (Sigma, St Louis, MA). cDNA was synthesized from 100 ng total RNA using iScript cDNA Synthesis Kit (Bio-Rad, Hercules, CA).

cDNA containing the region of interest (1287ins3) was amplified using primers that flank the mutation, *PLEC1* exon 9 forward (gatgaattcgagctgcagctgcg) and *PLEC1* exon 10 reverse (ctccaggattggtagatgcccttgg). Sequence analysis verified that the correct product was generated.

Normalization was performed with the housekeeping gene *GAPDH* as an internal control.

DNA Sequencing

DNA sequencing of 20 ng DNA/100 bp with 10 pmol of the respective primers was performed by MWG-Biotech.

SQRT-PCR

Primer combinations were tested by PCR of wild-type and patient cDNA to determine the best conditions for high specificity. SQRT-PCR was performed with Bio-Rad iCycler™ and Bio-Rad iQ™ SYBR Green Supermix Kit (Bio-Rad). Each primer of 15 pmol was added to the reactions. To minimize pipetting errors, reactions were prepared as master mixes. As a reference for semiquantitative analysis, we used the housekeeping gene *GAPDH*, after rejecting actin-β, RPLP0, and tubulin (*GAPDH*: forward, gccaacgtgtcagtggtgga; reverse, caccaccctgttgctgtagcc). For discriminiation between wild-type and mutated alleles a wild-type-specific forward primer for plectin exon 9 was designed. (PLEC1 exon 9 wt forward: gagctggtgctgctgctgcttcag PLEC1 exon 10 reverse: ctccagggattggtagatgcccttgg.)

cDNA (50 ng) from either PTM-transfected, mock-transfected EBS-MD, or wild-type fibroblasts were used for each reaction. Cycling conditions were 5 minutes at 95°C, 30 s at 95°C, 20 s at 65°C, 20 s at 72°C, followed by melt curve analysis (8 seconds each degree). Data were collected during each cycle and analyzed by the manufacturer's software. After the amplification, 5 μl of each real-time PCR product was analyzed on an agarose gel.

Cross-gene PCR analysis for plectin and related plakin genes

Genes of the plakin gene family encode desmoplakin, envoplakin, epiplakin, dystonin, periplakin, and microtubule-actin crosslinking factor 1. Possible illegitimate PTM-binding sites in each of those genes were identified using the MultAlin sequence alignment tool. Intronic sequences of the plakin genes were aligned with the sequence of the PTM-binding site located in intron 9 of *PLEC1*. Several possible PTM-binding sites in each plakin gene, as well as another binding site further downstream in the plectin gene were obtained. Specific reverse exonic primers downstream of the putative PTM-binding sites in the plakin genes were designed and PCR analysis in combination with a forward primer specific to plectin exon 9 was performed. A reverse primer for plectin exon 10 was added to the reaction mix to act as a positive control. PCR analysis was performed on cDNA from PTM-transfected and non-transfected EBS-MD fibroblasts.

Isolation of total protein from cultured cells

Cells were washed three times with phosphate-buffered saline and scraped off with a cell scraper. After centrifugation, cells were resuspended in 200 μl cell lysis buffer (0.5 M Tris–HCl, pH 6.8, 20% glycine, 10% SDS, 5% β-mercaptoethanol, and 1× complete protease inhibitor cocktail; Roche, Mannheim, Germany). The lysate was passed through a 22G syringe several times to disrupt cell aggregations and incubated at 95°C for 10 minutes.

Immunofluorescence

Cells were grown to about 75% confluency and fixed with 4% formaldehyde in phosphate-buffered saline. Cells were blocked for 1 hour with 10% normal swine serum, 0.1% BSA, 0.5% Triton X-100, and then incubated with 1:4 diluted mouse-derived mAb 5B3 to plectin (12). Biotin-labeled anti-mouse IgG antibody was used as a secondary antibody (Bio-Rad, Hercules) and visualized with cyanine-3-streptavidin conjugate from Amersham Pharmacia (Uppsala, Sweden).

Western blot analysis

SDS-PAGE. Total protein concentrations were determined by Bradford Assay (Bio-Rad) and equal amounts were applied on a 10% NuPAGE Bis-Tris-Gel (Invitrogen). Gels were run for 1 hour at 160 V. Proteins were blotted onto Hybond ECL 7 × 8 cm membranes (Amersham Pharmacia) for 1 hour at 0.8 A. After blocking for 1 hour with blocking buffer (200 mmol Tris–HCl, pH 7.6, 137 mmol NaCl, 0.2% I-Block (w/v), 0.1% Tween-20 (v/v)), mouse-derived mAb 5B3 diluted 1:4 in blocking buffer was added, and the membrane was incubated overnight at 4°C. Subsequent washing with blocking buffer was followed by incubation with 1:3,000 diluted alkaline phosphatase-linked anti-mouse-IgG (Sigma) for 1.5 hours. Specific bands were visualized with CDP-Star reagent from New England Biolabs.

The study was conducted according to the institutional regulation of experiments and adherence to the Declaration of Helsinki Principles.

CONFLICT OF INTEREST

Lloyd G. Mitchell is shareholder in a *trans*-splicing/gene-therapy company.

ACKNOWLEDGMENTS

This work was supported by DEBRA International and DEBRA Austria. Hanns Lochmueller is a member of the German network on muscular dystrophies (*MD-NET*, 01GM0302), funded by the German Ministry of Education and Research (BMBF, Bonn, Germany).

REFERENCES

Bauer JW, Rouan F, Kofler B, Rezniczek GA, Kornacker I, Muss W *et al.* (2001) A compound heterozygous one amino-acid insertion/nonsense mutation in the plectin gene causes epidermolysis bullosa simplex with plectin deficiency. *Am J Pathol* 158:617–25

Chao H, Mansfield SG, Bartel RC, Hiriyanna S, Mitchell LG, Garcia-Blanco MA *et al.* (2003) Phenotype correction of hemophilia A mice by spliceosome-mediated RNA *trans*-splicing. *Nat Med* 9:1015–9

Chao H, Walsh CE (2006) RNA repair for haemophilia A. *Expert Rev Mol Med* 8:1–8

Dallinger G, Puttaraju M, Mitchell LG, Yancey KB, Yee C, Klausegger A *et al.* (2003) Development of spliceosome-mediated RNA *trans*-splicing (SMaRT) for the correction of inherited skin diseases. *Exp Dermatol* 12:37–46

Foisner R, Feldman B, Sander L, Seifert G, Artlieb U, Wiche G (1994) A panel of monoclonal antibodies to rat plectin: distinction by epitope mapping and immunoreactivity with different tissues and cell lines. *Acta Histochem* 96:421–38

Kierlin-Duncan MN, Sullenger BA (2007) Using 5′ PTMs to repair mutant β-globin transcripts. *RNA* 13:1–11

Lai CH, Chun HH, Nahas SA, Mitui M, Gamo KM, Du L *et al.* (2004) Correction of ATM gene function by aminoglycoside-induced read-through of premature termination codons. *Proc Natl Acad Sci* 101:15676–81

Liu X, Jiang Q, Mansfield SG, Puttaraju M, Zhang Y, Zhou W *et al.* (2002) Partial correction of endogenous DeltaF508 CFTR in human cystic fibrosis airway epithelia by spliceosome-mediated RNA *trans*-splicing. *Nat Biotechnol* 20:47–52

Mansfield SG, Clark RG, Puttaraju M, Kole J, Cohn JA, Mitchell LG *et al.* (2003) 5′ Exon replacement and repair by spliceosome-mediated RNA *trans*-splicing. *RNA* 9:1290–7

Miller AD, Rosman GJ (1989) Improved retroviral vectors for gene transfer and expression. *Biotechniques* 7:980–90

Puttaraju M, Jamison SF, Mansfield SG, Garcia-Blanco MA, Mitchell LG (1999) Spliceosome mediated targeted *Trans*-splicing, a new tool for gene therapy and RNA repair. *Nat Biotechnol* 17:246–52

Puttaraju M, Yang Y, Spindler JE, Wang J, Cote CA, Ke W *et al.* (2004) High capacity screen to select optimal pre-*trans*-splicing molecules for *trans*-splicing applications. *Mol Ther* 9(Suppl 1):271–2 (abstr. 711)

Rezniczek GA, Abrahamsberg C, Fuchs P, Spazierer D, Wiche G (2003) Plectin 5′-transcript diversity: short alternative sequences determine stability of gene products, initiation of translation and subcellular localization of isoforms. *Hum Mol Genet* 12:3181–94

Tahara M, Pergolizzi RG, Kobayashi H, Krause A, Luettich K, Lesser ML *et al.* (2004) *Trans*-splicing repair of CD40 ligand deficiency results in naturally regulated correction of a mouse model of hyper-IgM X-linked immunodeficiency. *Nat Med* 10:835–41